J|A|C|S
ARTICLES
Published on Web 02/07/2002

Interaction of Biotin with Mg−O Bonds: Bifunctional Binding and Recognition of Biotin and Related Ligands by the Mg(15-crown-5)$^{2+}$ Unit

Elizabeth R. Sanchez, Mary C. Gessel, Thomas L. Groy, and M. Tyler Caudle*

Contribution from the Department of Chemistry and Biochemistry, Arizona State University, Box 871604, Tempe, Arizona 85287-1604

Received July 17, 2001

Abstract: The interaction between biotin and the macrocyclic magnesium complex Mg(15-crown-5)(Otf)$_2$ (15-crown-5 is 1,4,7,10,13-pentaoxacyclopentadecane, Otf$^-$ is trifluoromethanesulfonate anion) in solution was studied as a model for metal−biotin interactions that may be important in its speciation and function. Shifts in the solution IR spectrum establish that the interaction is dominated by ligation between the carbonyl oxygen of the ureido ring of biotin and the Mg^{2+} cation. However, comparative binding studies using NMR spectroscopy and conductivity reveal a substantial enthalpic contribution to binding that arises from interactions between the ureido −NH moiety and the macrocyclic ring. This is interpreted in terms of a weak-to-moderate hydrogen bond formed between the −NH group and an oxygen from the crown, which is simultaneously coordinated to Mg^{2+}. This hypothesis is reinforced by quantitative examination of the binding of N-methylated derivatives of 2-imidazolidone, which shows that N,N'-dimethylation decreases the affinity of Mg(15-crown-5)(Otf)$_2$ for the ligand by 2 orders of magnitude. This can be understood in terms of the structure of Mg(15-crown-5)(Otf)$_2$. It shows a pentagonal bipyramidal coordination geometry where the five equatorial positions are occupied by the macrocyclic oxygen donors. The axial positions are occupied by weakly coordinating Otf$^-$ anions, which are readily displaced by biotin and related derivatives. The Mg−O$_{crown}$ bond distance ranges from 2.1 to 2.3 Å, providing structural complementarity for the 2.2 Å C═O···HN− bite distance in the ureido group, which leads to strong interaction. The contribution from hydrogen bonding illustrates the importance of second-shell interactions in the biocoordination chemistry of Mg^{2+}. These can serve to organize cofactor interactions with biomolecules, as was recently demonstrated for a biotin-selective RNA aptamer that depends on a direct biotin−magnesium interaction for recognition of biotin (Nix, J.; Sussman, D.; Wilson, C. *J. Mol. Biol.* **2000**, *296*, 1235−1244). These results are significant in the context of the observed magnesium requirement in biotin-dependent carboxylase enzymes, where noncovalent interactions with biotin may be important in its activation toward carboxylation in the first step of biotin-dependent CO_2 transfer. The synthetic system presented here also suggests that the Mg−O bond may be considered a constituent design element in the rational preparation of complexes to bind and recognize biotin.

Biotin, **1**, is the critical cofactor in biotin-dependent carboxylase (BDC) enzymes, whose chemical function is the fixation of carbon dioxide from bicarbonate.[1] Turnover of the enzyme involves initial generation of N^1-carboxybiotin by CO_2 transfer from bicarbonate, Scheme 1, which is carried out by the biotin carboxylase subunit and requires two equivalents of Mg^{2+} ion as inorganic cofactors.[2] While the biotin carboxylase subunit has been structurally characterized in its apo forms,[3] these structures are not informative about the specifics of biotin binding leading to carboxylation. The chemical mechanism of carboxylation has therefore attracted considerable speculation, particularly regarding how biotin, a poor nucleophile, is induced to react with bicarbonate, a poor electrophile. This is presumed to proceed via deprotonation of the N^1 site on biotin, followed by reaction with a CO_2 equivalent generated from bicarbonate.

Scheme 1

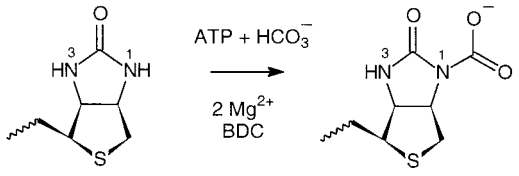

1

* To whom correspondence should be addressed.

(1) Knowles, J. R. *Annu. Rev. Biochem.* **1989**, *58*, 195−221. Jitrapakdee, S.; Wallace, J. C. *Biochem. J.* **1999**, *340*, 1−16. Attwood, P. V. *Int. J. Biochem. Cell Biol.* **1995**, *27*, 231−249.

(2) Werneburg, B. G.; Ash, D. *Biochemistry* **1997**, *36*, 14392−14402. Goodall, G. J.; Baldwin, G. S.; Wallace, J. C.; Keech, D. B. *Biochem. J.* **1981**, *199*, 603−609. Attwood, P. V.; Wallace, J. C.; Keech, D. B. *Biochem. J.* **1984**, *219*, 243−251. Branson, J. P.; Attwood, P. V. *Biochemistry* **2000**, *39*, 7480−7491. Attwood, P. V. *Biochem. Soc. Trans.* **1998**, *26*, 6, S174. Attwood, P. V.; Graneri, B. D. L. A. *Biochem. Soc. Trans.* **1991**, *19*, 231S. Attwood, P. V.; Wallace, J. C. *Biochem. J.* **1986**, *235*, 359−364.

(3) Waldrop, G. L.; Rayment, I.; Holden, H. M. *Biochemistry* **1994**, *33*, 10249−10256. Thoden, J. B.; Blanchard, C. Z.; Holden, H. M.; Waldrop, G. L. *J. Biol. Chem.* **2000**, *275*, 16183.

Scheme 2

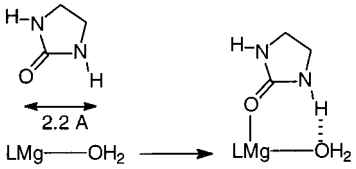

However, this mechanism generates two chemical problems for the enzyme. First, the aqueous pK_a of the $-N^1H$ proton on biotin is 17.4,[4] which requires either an unusually strong active site base or a means for decreasing the pK_a of biotin. Second, the buildup of local negative charge upon deprotonation of biotin needs to be minimized. In principle, both of these problems could be alleviated by coordination of the biotin to a Lewis acidic metal cation, which suggests one possible role for magnesium in carboxyl transfer in BDC enzymes.

There have been few studies systematically addressing the coordination chemistry of biotin[5] and related cyclic ureas[6] that would provide a chemical framework for understanding metal−biotin interactions, and no studies address second-shell interactions that are apt to be important in magnesium−biotin complexes. The importance of second-shell interactions was recently demonstrated in a biotin-selective RNA aptamer that showed the biotin headgroup directly ligated to a hydrated magnesium ion.[7,8] The biotin guest is organized partly by close interactions with the magnesium ion's hydration sphere, suggesting an important role for hydrated Mg^{2+} in biotin recognition. This highlights a need for systematic chemical studies to probe factors leading to efficient biotin binding to magnesium. Mg^{2+} is often bound by biomolecules in a highly hydrated state when compared to transition-metal cations, and interactions with Mg^{2+} waters of hydration are generally critical in magnesium/protein and magnesium/polynucleotide interactions.[9] In addition, hydrated Mg^{2+} may play specific roles in the recognition and orientation of enzyme substrates and cofactors in Mg^{2+}-dependent enzymes such as the biotin-dependent carboxylases.

We have sought to understand biotin interactions with magnesium by employing the model of bifunctional binding that has been successful in the design of organic receptors for the biotin headgroup.[10] This has typically involved positioning a carboxylic acid group so that its Lewis acidic −OH and Lewis basic C═O interact simultaneously with the carbonyl oxygen and the ureido −NH groups of biotin, respectively. The "bite" distance between the Lewis acidic proton and Lewis basic carbonyl oxygen of the carboxylic acid is 2.3 Å, a good structural match for the ureido group of biotin, which has a C═O···HN− bite of about 2.2 Å,[11] Scheme 2. A receptor in which the Lewis acidic site is replaced by Mg^{2+} should then provide a Lewis basic site approximately 2.2−2.3 Å away. This criteria is generally satisfied by magnesium−oxygen bonds, as exemplified by the 2.1 Å Mg−O bond in $Mg(OH_2)_6^{2+}$.[12]

The detailed elucidation of molecular interactions with Mg^{2+} hydrates has proven a challenge, partly as a result of the general lability of the water ligands and the dearth of convenient spectroscopic probes for determining the degree of binding. The problem of lability can be overcome by the use of oxygen-donor macrocyclic ligands that bind Mg^{2+} tightly and exchange slowly. This provides a kinetically stable frame of reference for establishing biotin binding to the complex. The complexes of 15-crown-5 (1,4,7,10,13-pentaoxacyclopentadecane) with magnesium exhibit $Mg-O_{crown}$ bond lengths of about 2.2 Å,[13] similar to the $Mg-OH_2$ bond length, and yet provide a vacant coordination site for biotin binding. A lone pair of electrons on the coordinated O_{crown} can then provide the requisite basic site for hydrogen bonding to the ureido group, so that biotin−Mg-(15-crown-5)$^{2+}$ complexes should be an effective model for interactions between hydrated Mg^{2+} and biotin. This basic design principle is supported by examination of the crystal structures of simple magnesium−urea complexes,[14] which commonly exhibit hydrogen bonding between the −NH bond of a coordinated urea and an oxygen donor situated -*cis* to it with an $Mg-O_{cis}$ distance of 2.1−2.2 Å.

In this paper, we characterize the binding of the biotin ethyl ester to Mg(15-crown-5)$(Otf)_2$ (Otf^- is trifluoromethanesulfonate anion). The impetus for this work is to develop a more sophisticated understanding of noncovalent interactions with biotin that may contribute to its molecular recognition and chemical activation. The crown ether reduces the number of labile coordination sites when compared to simple solvated magnesium cations and permits more control over the binding orientation and stoichiometry. The macrocyclic ligand also provides opportunity for additional functionality to recognize biotin through hydrogen-bonding interaction with the crown oxygen atoms, which should increase the stability of the biotin−Mg^{2+} adducts in solution. To better understand structural factors involved in biotin binding to the simple magnesium-based receptors, we have also characterized binding of a series of related analogues, Scheme 3, which provided important insight into factors affecting the binding stability and specificity.

Experimental Section

Materials and Equipment. The ligands 2-imidazolidone (**3**), *N*-methyl-2-imidazolidone (**5**), *N*,*N*′-dimethyl-2-imidazolidone (**6**), 2-pyrolidinone (**7**), and cyclopentanone (**8**) were recrystallized or vacuum distilled before use and stored under nitrogen. The ligand 4,4-dimethyl-2-imidazolidone (**4**) was synthesized as described below. Magnesium trifluoromethansulfonate, $Mg(Otf)_2$, was stored under nitrogen and 15-crown-5 was stored under nitrogen with 4A molecular sieves. (+)-

(4) Fry, D. C.; Fox, T. L.; Lane, M. D.; Mildvan, A. S. *J. Am. Chem. Soc.* **1985**, *107*, 7659−7665.
(5) Sigel, H.; McCormick, D. B.; Griesser, R.; Prijs, B.; Wright, L. D. *Biochemistry* **1969**, *8*, 2687−2695. Griesser, R.; Sigel, H.; Wright, L. D.; Mccormick, D. B. *Biochemistry* **1973**, *12*, 1917−1923. Kondo, H.; Miura, K.; Uno, S.; Sunamoto, J. *J. Inorg. Biochem.* **1984**, *21*, 93−102. Kondo, H.; Horiguchi, D.; Ikeda, S.; Sunamoto, J.; Tsujii, K. *J. Org. Chem.* **1979**, *44*, 4430−4435.
(6) Reedjik, J.; Mulder, T. M.; Smit, J. A. *Inorg. Chim. Acta* **1975**, *13*, 219−227.
(7) Nix, J.; Sussman, D.; Wilson, C. *J. Mol. Biol.* **2000**, *296*, 1235−1244.
(8) Wilson, C.; Nix, J.; Szostak, J. *Biochemistry* **1998**, *37*, 14410−14419.
(9) Black, C. B.; Cowan, J. A. In *The biological chemistry of magnesium*; Cowan, J. A., Ed.; VCH Publishers: New York, 1995; pp 159−183. Dudev, T.; Cowan, J. A.; Lim, C. *J. Am. Chem. Soc.* **1999**, *121*, 7665−7673.
(10) Adrian, J. C., Jr.; Wilcox, C. S. *J. Am. Chem. Soc.* **1989**, *111*, 8055−8057. Rao, P.; Maitra, U. *Supramol. Chem.* **1998**, *9*, 325−328.
(11) DeTitta, G. T.; Edmonds, J. W.; Stallings, W.; Donahue, J. *J. Am. Chem. Soc.* **1976**, *98*, 1920−1926.
(12) Braibanti, A.; Tiripicchio, A.; Manotti-Lanfredi, A. M.; Bigoli, F. *Acta Crystallogr., Sect. B* **1969**, *25*, 354−361. Bock, C. W.; Kaufman, A.; Glusker, J. P. *Inorg. Chem.* **1994**, *33*, 419−427.
(13) Chadwick, S.; Englich, U.; Ruhlandt-Senge, K. *Inorg. Chem.* **1999**, *38*, 6289−6293. Rubtsova, T. B.; Kireeva, O. K.; Bulychev, B. M.; Streltsova, N. P.; Belsky, V. K.; Tarasov, B. P. *Polyhedron* **1992**, *11*, 1929−1938. Owen, J. D. *J. Chem. Soc., Dalton Trans.* **1978**, 1418−1423.
(14) Todorov, T.; Petrova, R.; Kossev, K.; Macicek, J.; Angelova, O. *Acta Crystallogr., Sect. C* **1998**, *54*, 1758−1760. Todorov, T.; Petrova, R.; Kossev, K.; Macicek, J.; Angelova, O. *Acta Crystallogr., Sect. C* **1998**, *54*, 456−458. Lebioda, L.; Lewinski, K. *Acta Crystallogr., Sect. B* **1980**, *36*, 693−695. Hayden, T. D.; Kim, E. E.; Eriks, K. *Inorg. Chem.* **1982**, *21*, 4054−4058.

Scheme 3

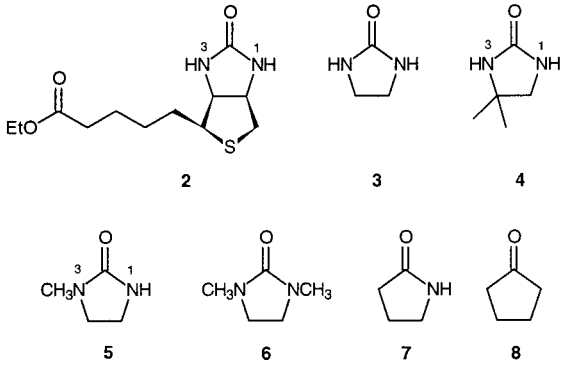

2 **3** **4** **5** **6** **7** **8**

Biotin was purchased from Aldrich and esterified as described below. Acetonitrile and acetonitrile-d_3 used in analytical procedures were purified by stirring over anhydrous copper sulfate/calcium hydride for 24 h and then by distilling over phosphorus pentoxide. Solvents used in preparative procedures were purified according to standard methods. All analytical manipulations were carried out under nitrogen to minimize contact of the solutions and materials with water.

Temperature-dependent NMR spectra were run on a Varian Unity 400 MHz instrument. Routine infrared spectra were measured on a Nicolet Avatar 360 FTIR instrument. Solution IR were recorded using a flow cell with potassium bromide windows.

Biotin Ethyl Ester (2). 1.0 g of (+)-biotin was slurried in 25 mL 95% ethanol. Three drops of concentrated hydrochloric acid were added and the mixture was refluxed for 8 h. The volume of the clear solution was reduced 50% by distillation. The remaining solution was removed in vacuo to give a white flaky residue. This material was dissolved in 20 mL acetone and eluted through a 19 × 2.5 cm column of silica gel using acetone as the eluting solvent. The first 700 mL of eluate was collected and reduced in volume to 25 mL by rotary evaporation. The solution was treated with a small amount of activated charcoal, filtered, and evaporated to dryness to give 0.60 g (54%) of pure biotin ethyl ester **2**. IR (cm^{-1}, KBr): 3239 s, 2925 m, 1730 s, 1707 s, 1477 m, 1284 m, 1212 m, 1026 w. ^1H NMR (ppm, CD_3CN): 5.32(singlet), 5.20-(singlet), 4.43(multiplet), 4.26(multiplet), 4.10(quintet), 3.18(multiplet), 2.91(multiplet), 2.66(multiplet), 2.31(triplet), 1.62(multiplet), 1.42-(multiplet), 1.23(triplet). Compositional analysis found(calc)%: C, 52.9-(52.9); H, 7.7(7.4); N, 10.2(10.3); S, 11.4(11.8).

4,4-Dimethyl-2-imidazolidone (4). 3.23 mL (30.8 mmol) 1,2-diamino-1,1-dimethyl-propane and 5.0 g (30.8 mmol) 1,1-carbonyldi-imidazole were refluxed for 24 h in anhydrous THF under N_2. Evaporation of the solvent gave a yellow oil which was dissolved in water. The pH was adjusted to 2 and the aqueous solution was extracted with CH_2Cl_2. The collected organic layer was evaporated to dryness to give a white solid. Recrystallizing from hexane/THF provided 1.81 g (53%) pure **4** as a white crystalline powder. mp 101−104 °C; IR (cm^{-1}, KBr): 3233 s, 2968 m, 1713 s, 1305 m, 1205 w, 717 m, 555 w. ^1H NMR (ppm, CD_3CN): 4.97(singlet), 4.78(singlet), 3.15(singlet), 1.26-(singlet). Compositional analysis found (calc)%: C, 52.4(52.6); H, 8.5-(8.8); N, 24.0(24.5).

Mg(15-crown-5)(Otf)$_2$. 5.94 g (18.4 mmol) magnesium trifluoromethanesulfonate and 3.66 mL (18.4 mmol) 15-crown-5 were combined in 75 mL anhydrous acetonitrile in a sealed heavy-wall pressure flask and heated to 80 °C for 1 h, after which all of the magnesium salt had dissolved. The solution was cooled and filtered. The solvent was evaporated under a stream of nitrogen to give a white microcrystalline solid which was washed twice with 20% (v/v) acetonitrile in diethyl ether and then was washed with pure diethyl ether. Drying in vacuo gave 9.23 g (92% yield) Mg(15-crown-5)(Otf)$_2$. X-ray quality crystals were prepared by permitting diethyl ether vapor to slowly diffuse into an acetonitrile solution of Mg(15-crown-5)(Otf)$_2$ under strictly anhydrous conditions.[15] IR (cm^{-1}, KBr): 1481 w, 1310 m, 1252 m, 1167 m, 1092 s, 1040 s, 972 m, 638 s. ^1H NMR (ppm, CD_3CN) 3.89(singlet, broad). Compositional analysis found (calc)%: C, 26.5(26.6); H, 3.7(3.7); N, 0(0); S, 12.1(11.8).

Table 1. Crystallographic Data for Mg(15-crown-5)(Otf)$_2$

formula	$C_{12}H_{20}F_6MgO_{11}S_2$
formula weight	542.71
crystal system	monoclinic
space group	$P2_1/n$
color	colorless
a	8.5567(7) Å
b	9.7163(8) Å
c	13.4190(11) Å
α	90.00°
β	101.6220(10)°
γ	90.00°
V	1092.78(16) Å^3
Z	2
temperature	173(2) K
λ	0.71073 Å
measured reflections	10398
independent reflections	2512
observed reflections	1896
R_{all}	0.0691
R_{obs}	0.0551
wR_{all}	0.1709
wR_{obs}	0.1603
GOF	1.071

Crystallography. A suitable crystal of Mg(15-crown-5)(Otf)$_2$ was coated in mineral oil and mounted in a sealed glass capillary for X-ray diffraction on a Bruker SMART APEX. Structure solution and refinement were performed using SHELXS-97 and SHELXL-97. Refer to Table 1 and Supporting Information for additional details of data collection and refinement.

NMR Titration Studies. The desired ligand **2-8** was dissolved in CD_3CN, and 1 μL of benzene was added as an internal concentration standard, which was then used to determine the precise concentration of the ligand. A stock solution of about 100 mM Mg(15-crown-5)-(Otf)$_2$ was prepared in CD_3CN. This solution was added in aliquots to the ligand solution, and the proton NMR spectrum was measured after each addition. The binding ratio $[L]_b/[L]_{tot}$ ($[L]_b$ = bound ligand concentration, $[L]_{tot}$ = total ligand concentration) was calculated from the NMR spectrum and plotted against $[Mg(15\text{-crown-}5)]_{tot}/[L]_{tot}$.

Conductivity Studies. A YSI conductivity dip probe was calibrated in acetonitrile using tetrabutylammonium bromide as a standard 1:1 electrolyte, which gave a cell constant of 1.3 μS/cm. The calibrated probe, interfaced to an Accumet 50 pH/ion/conductivity meter, was used to measure the solution conductivity κ of Mg(15-crown-5)(Otf)$_2$ in the presence of differing amounts of added ligand. The apparent molar conductance Λ_M was calculated by the relationship $\Lambda_M = \kappa/c$, where c is the concentration of Mg(15-crown-5)(Otf)$_2$. The temperature was not permitted to fluctuate more than ±3 °C during the course of the measurements. All conductivity measurements were made inside a drybox to eliminate absorption of atmospheric moisture, which was observed to increase the measured conductivity.

Results and Discussion

The molecular structure of Mg(15-crown-5)(Otf)$_2$ is presented in Figure 1. It shows the expected pentagonal plane of the macrocyclic ring, with two Otf^- anions in axial positions above and below. The topology is similar to previously characterized $Mg(15\text{-crown-}5)^{2+}$ complexes.[13] The $Mg-O_{crown}$ bond lengths

(15) Crystals of the dihydrate, $[Mg(15\text{-crown-}5)(OH_2)_2][Otf]_2$ were consistently isolated when no precautions were taken to exclude moisture. The crystals of the dihydrate were of poor diffraction quality, but minimal connectivity was determined by X-ray diffraction. This clearly showed that the Otf^- anions had been displaced from the magnesium ion by water ligands.

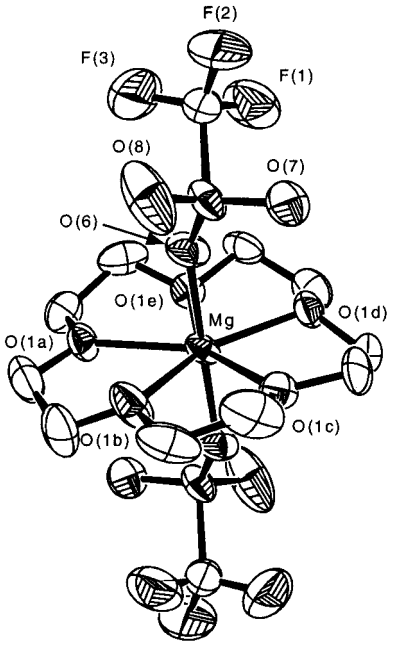

Figure 1. Molecular structure of Mg(15-crown-5)$(Otf)_2$ (50% probability ellipsoids). Important bond lengths (Å). Mg−O(1a), 2.228(4); Mg−O(1b), 2.263(5); Mg−O(1c), 2.115(3); Mg−O(1d), 2.136(3); Mg−O(1e), 2.184(3); Mg−O(6), 2.045(2). Important bond angles (°): O(6)−Mg−O(1a), 94.19(12); O(6)−Mg−O(1b), 87.82(15); O(6)−Mg−O(1c), 93.39(11); O(6)−Mg−O(1d), 87.02(12); O(6)−Mg−O(1e), 92.19(10).

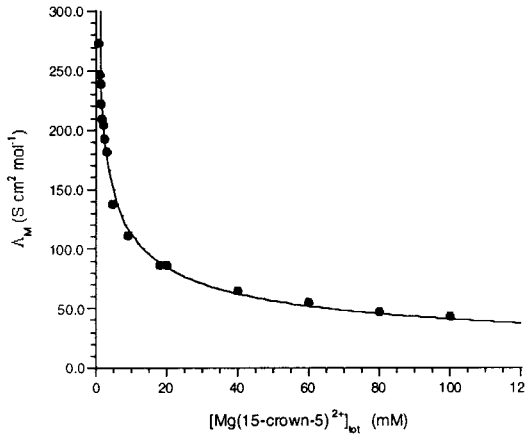

Figure 2. Apparent molar conductance for Mg(15-crown-5)$(Otf)_2$ in CH_3CN. Molar conductance was measured at 25 °C for solutions varying in concentration of Mg(15-crown-5)$(Otf)_2$. The best fit of the data to eq 1 gives $K_{i(1)} = 0.016(2)$ M and $K_{i(2)} = 0.0017(3)$ M.

range between 2.115 and 2.263 Å, well within the expected range for these complexes. The Mg−O(6) bond is somewhat shorter, 2.045 Å, a result of the anionic charge on the Otf^- ligand. The macrocycle oxygen atoms lie nearly in a plane, as indicated by the fact that the sum of the O−Mg−O bond angles is 360°. The axial Otf^- ligands are tilted slightly with respect to the MgO_5 plane. The only unusual features of the structure are large thermal parameters for F(3) and O(8), which may be attributable to close interactions with adjacent molecules of Mg(15-crown-5)$(Otf)_2$.

Mg(15-crown-5)$(Otf)_2$ is distinguished by the presence of the labile trifluoromethanesulfonate anions in the axial positions. In CH_3CN solution, Mg(15-crown-5)$(Otf)_2$ behaves as a weak electrolyte, indicated by a curved plot of apparent molar conductance, Λ_M, with concentration, Figure 2. Both Otf^- anions

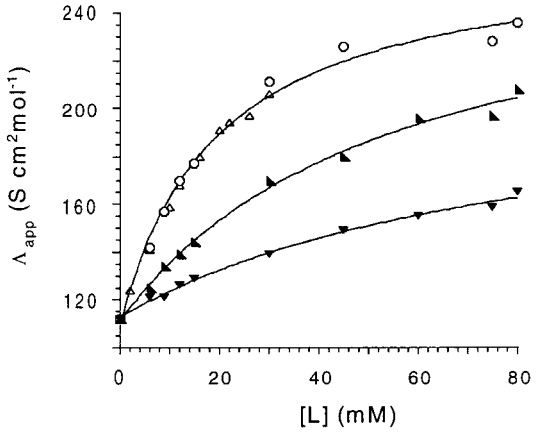

Figure 3. Apparent molar conductance (CH_3CN) of Mg(15-crown-5)$(Otf)_2$ as a function of added ligand. [Mg(15-crown-5)$(Otf)_2$] = 0.010 M, $T = 25$ (±3)°C. Solid lines show trend in the data. △ = **3**, ○ = **4**, ▼ = **6**, ▲ = **7**.

are displaced at concentrations below 10 mM, and Mg(15-crown-5)$(Otf)_2$ behaves as a 2:1 electrolyte. At concentrations greater than 20 mM, only one Otf^- is displaced. Assuming stepwise ionization equilibria with $K_{i(1)} \gg K_{i(2)}$ permits derivation of a combined ionization isotherm relating apparent molar conductance, Λ_M, to [Mg(15-crown-5)$^{2+}$]$_{tot}$, Eq 1.[16] The best fit of the conductance data in Figure 2 gives estimates for the ionization equilibrium constants $K_{i(1)} = 0.016(2)$ M and $K_{i(2)} = 0.0017(3)$ M in CH_3CN. The lability of the Otf^- anions in Mg(15-crown-5)$(Otf)_2$, which provides two *-trans* coordination sites for exogeneous ligands, and the appropriate 2.2 Å Mg−O_{crown} bond distance therefore satisfy the initial design criteria for a magnesium-based biotin binding motif.

$$\Lambda_M = \Lambda_1 \frac{-K_{i(1)} + [K_{i(1)}{}^2 - 4a_oK_{i(1)})]^{1/2}}{2a_o} + \Lambda_2 \frac{-(a_o + K_{i(2)}) + [(a_o + K_{i(2)})^2 - 4a_oK_{i(2)})]^{1/2}}{2a_o} \quad (1)$$

a_o = [Mg(15-crown-5)$^{2+}$]$_{tot}$

Λ_1 = molar conductance of 1:1 electrolyte

Λ_2 = molar conductance of 2:1 electrolyte − Λ_1

Since generation of a coordination site on Mg(15-crown-5)$(Otf)_2$ involves displacement of a Otf^- anion, conductivity can be used to qualitatively probe the binding equilibrium. At 10 mM, Λ_M for Mg(15-crown-5)$(Otf)_2$ is 112 S·cm^{2}mol^{-1}, which is consistent with a 1:1 electrolyte[17] and indicates that one equiv of Otf^- is dissociated on average. Addition of ligand **4** to the solution increases Λ_M, and saturation behavior is observed as [**4**] is increased, Figure 3. The saturating molar conductance, Λ_{max}, of about 250 S·cm^{2}mol^{-1} is higher than the value expected for a 1:1 electrolyte (120−160) and in the lower range of values expected for a 2:1 electrolyte (220−350) in CH_3CN.[17] This indicates that under conditions of 10 mM Mg(15-crown-5)$(Otf)_2$, one Otf^- anion is completely displaced by **4** and a second is partially displaced. Figure 3 also demonstrates a clear difference in the affinities of the ligands for Mg(15-crown-5)$(Otf)_2$. Ligands **3** and **4** compete more effectively with Otf^- for the binding

(16) Derivation of this equation is deposited as supporting material.
(17) Geary, W. J. *Coord. Chem. Rev.* **1971**, *7*, 81−122.

Scheme 4

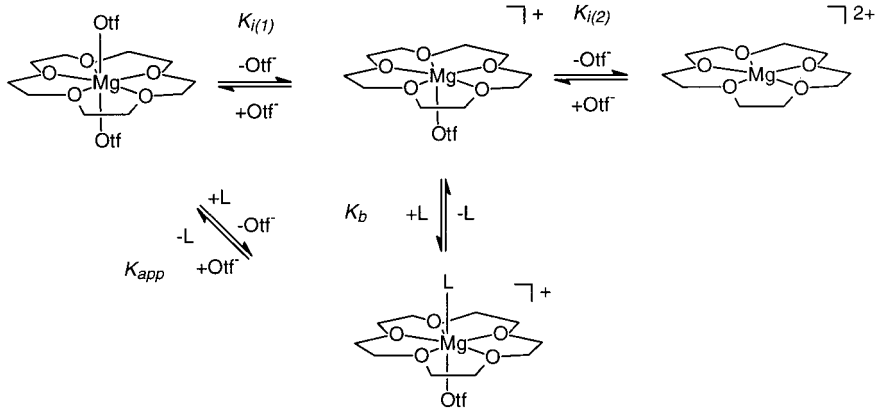

site than the N,N'-dimethylated counterpart **6** and the lactam derivative **7**. This points to a structural basis for the binding affinity since **6**, though expected to be a slightly stronger Lewis base than **7**, nevertheless binds more weakly. On the basis of the conductance measurements, the binding equilibrium is consistent with Scheme 4, in which K_b is the binding constants for interaction of the ligand L with the Mg(15-crown-5)$^{2+}$ unit and $K_{i(n)}$ are the ionization constants resulting from displacement of Otf$^-$ anions.

The binding mode of ligands **2**−**8** was probed using solution FTIR spectroscopy, which strongly supports ligation to the Mg^{2+} ion via the ureido carbonyl oxygen. For example, the stretching frequency of the ureido group in **5** appears at $\nu_{max} = 1709$ cm^{-1} in CH_3CN solution. Incremental addition of Mg(15-crown-5)-$(Otf)_2$ results in the appearance of a new infrared absorption peak at $\nu_{max} = 1685$ cm^{-1}, Figure 4. These data show that the ureido stretching frequency shifts to lower energy ($\Delta_{\nu max} = 24$ cm^{-1}) in the presence of Mg(15-crown-5)$(Otf)_2$, consistent with a decrease in C═O bond order associated with ligation of the carbonyl oxygen to a metal ion. The isosbestic behavior of the spectra in this titration experiment shows the formation of a well-defined adduct, without buildup of any observable intermediates or alternate products. Similar shifts are observed for ligands **2**−**8** when bound to Mg(15-crown-5)$(Otf)_2$, although this effect is obscured somewhat in the case of **2** by the presence of the carbonyl group from the ester. However, it is significant that ν_{max} for free **2**, 1716 cm^{-1}, shifts to 1694 cm^{-1} ($\Delta_{\nu max} =$ 22 cm^{-1}) in the presence of Mg(15-crown-5)$(Otf)_2$. The essentially identical IR shifts are expected if the binding mode is the same for **2** and **5**. A weaker carbonyl band at 1729 cm^{-1}, arising from the ester group in **2**, does not shift at all in the presence of the magnesium complex, indicating no interaction with the ester. For the entire series of ligands, the IR data therefore point to a similar binding interaction between the ureido oxygen and the Mg^{2+} ion.

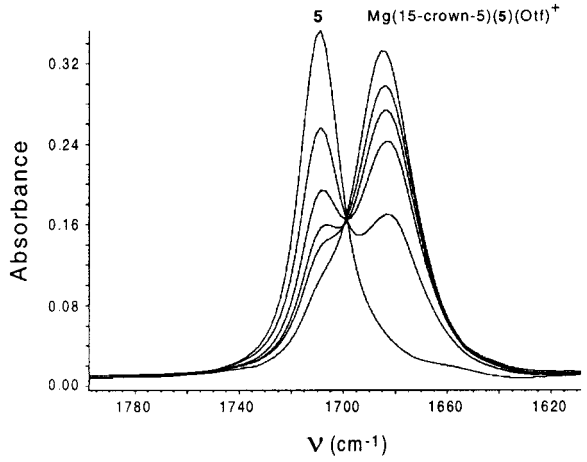

Figure 4. Solution infrared absorption spectra (CH_3CN) of **5** as a function of added Mg(15-crown-5)$(Otf)_2$. [**5**] = 30 mM. [Mg(15-crown-5)$(Otf)_2$] = 0−60 mM.

Because the conductivity and IR experiments were very consumptive of ligand, this method was not suitable for quantitative measurement of the binding affinity of **2** and the model ligands. However, the proton NMR spectrum of **2**, Figure 5a, is well-resolved and provides a means to efficiently monitor the binding to Mg(15-crown-5)$(Otf)_2$. Upon addition of the magnesium complex to a solution of **2** in CD_3CN, a new set of NMR signals appear in the heterocycle region downfield from the free biotin ethyl ester signals so that the spectrum of **2** in this region appears to be split. As the concentration of Mg(15-crown-5)$(Otf)_2$ increases, Figure 5b−e, the new signals increase in intensity at the expense of the original signals, until the signals from free biotin disappear altogether. The largest chemical shifts occur in the protons on the ureido ring of **2**, *a*−*f*, and there is a notable lack of shifting in the ester side chain signal *g*. This observation is consistent with the FTIR data in supporting a ureido binding mode.

There are two other qualitative observations apparent by inspection of Figure 5. First, chemical exchange between free and bound biotin is in the slow exchange NMR limit. Under conditions where the fraction of free **2** is equivalent to the fraction of bound **2**, Figure 5c, the half-height line width $\Delta\nu_{1/2}$ of a given resonance is related to the chemical exchange rate k_{ex} by eq 2,[18] where $\Delta\nu_{1/2}°$ is the half-height width in the absence of chemical exchange.

$$\Delta\nu_{1/2} = \Delta\nu_{1/2}° + k_{ex}/\pi \qquad (2)$$

Using this equation with measured values for $\Delta\nu_{1/2}$ (3.5 s^{-1}) and $\Delta\nu_{1/2}°$ (2.6 s^{-1}) for resonance *e*, we can estimate the rate for exchange between free and bound **2** to be about 3 s^{-1}. Although solvent exchange kinetics for Mg(15-crown-5)$^{2+}$ tends to be slow in nonaqueous donor solvents ($k_{ex} \approx 20$ s^{-1}),[19,20]

(18) Becker, E. D. *High-resolution NMR*; Academic Press: New York, 1980.
(19) Dickert, F. L.; Gumbrecht, W.; Hellmann, S. W.; Waidhas, M. F. *Ber. Bunsen-Ges. Phys. Chem.* **1985**, *89*, 875−879.
(20) Dickert, F. L.; Waidhas, M. F. *Angew. Chem., Int. Ed. Engl.* **1985**, *24*, 575−576.

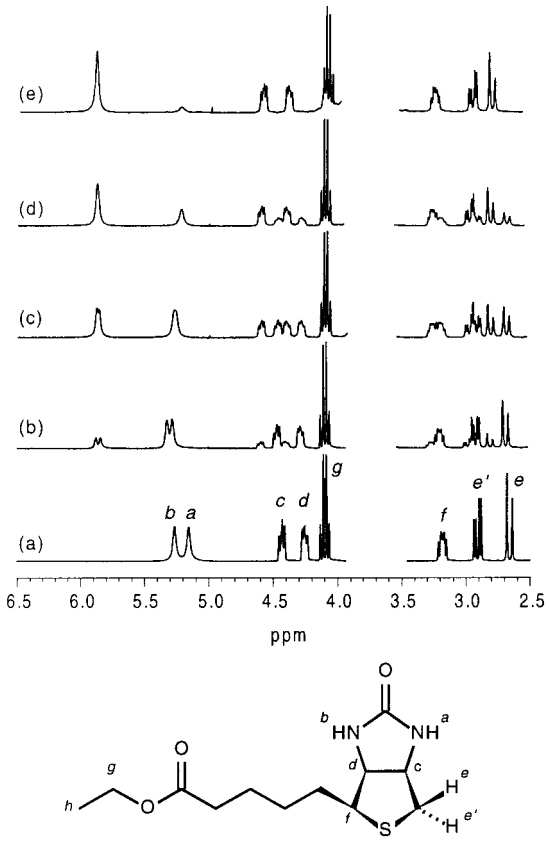

Figure 5. Proton NMR spectra (300 MHz, CD_3CN) of **2** as a function of added Mg(15-crown-5)$(Otf)_2$. NMR assignments from Bates and Rosenblum.[25] The excised region is where the resonance for Mg(15-crown-5)$(Otf)_2$ appears. [**2**] = 0.010 M. $[Mg(15\text{-crown-5})]_{tot}/[L]_{tot}$ = (a) 0; (b) 0.18; (c) 0.35; (d) 0.54; (e) 3.4.

the exchange of **2** is especially sluggish, suggesting that the crown ether imparts a degree of kinetic stability to these adducts. Second, the −NH protons in **2** shift downfield by 0.6 ppm upon binding to the crown complex and the $-N^1H$ and $-N^3H$ protons *a* and *b* coalesce. The chemical shift data show that the −NH protons reside in a substantially more electronegative chemical environment when bound to the Mg(15-crown-5)$^{2+}$. Coalescence could be interpreted to arise from an increase in the proton exchange rate between the N^1 and N^3 positions upon binding to Mg(15-crown-5)$^{2+}$, but we do not observe the inequivalent −NH protons in **4** to coalesce under the same conditions. It is therefore more reasonable that the coalescence in **2** results from accidental degeneracy of the −NH signals in the presence of the magnesium complex.

Integration of the proton NMR signals from free and bound ligand were used to measure the binding ratio $Q = [L]_b/[L]_{tot}$ ($[L]_b$ = concentration of bound ligand, $[L]_{tot}$ = total concentration of ligand). Figure 6 shows Q as a function of $[Mg(15\text{-crown-5})]_{tot}/[L]_{tot}$ ($[Mg(15\text{-crown-5})]_{tot}$ = total concentration of Mg(15-crown-5)$^{2+}$) for L = **2**−**7**. Ligand **8** bound so weakly that we were unable to determine binding ratios for its ligation. The plot shows saturation behavior with $Q_{max} = 1$, consistent with the formation of a 1:1 complex under these conditions. The data for Q as a function of $[Mg(15\text{-crown-5})]_{tot}/[L]_{tot}$ fits well to the theoretical 1:1 binding isotherm expression, eq 3.[16] This expression was used to fit the data in Figure 6 and derive estimates for the apparent binding constant K_{app}. Since the NMR spectra were measured under conditions where [Mg(15-crown-5)$(Otf)_2$] ≥ 10 mM, K_{app} is in fact a conditional equilibrium constant equal to $K_b \cdot K_{i(1)}$, Scheme 4. $K_{i(1)}$ is a constant, and so the magnitude of K_{app} is a measure of the relative affinity of Mg(15-crown-5)$(Otf)^+$ for the ligand L. Values are tabulated in Table 2 along with calculated values for K_b. These data show that K_{app} is critically dependent on the nature of the ligand. The factor of 350 variation in K_{app} shows that Mg(15-crown-5)$(Otf)_2$ has a degree of discrimination for binding structurally similar ligands, with the biotin ethyl ester **2** among the strongest binding in this series.

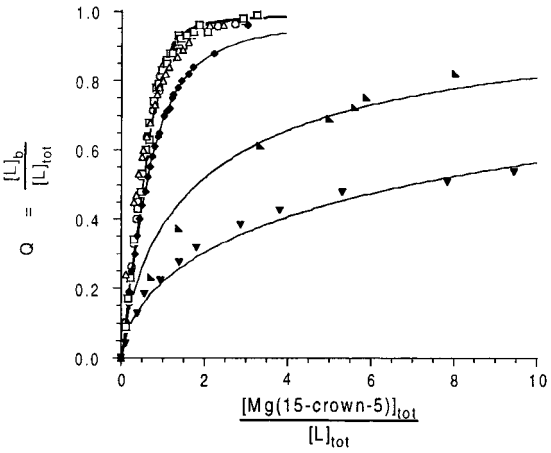

Figure 6. Binding ratio Q as a function of $[Mg(15\text{-crown-5})]_{tot}/[L]_{tot}$ for ligands **2**−**7** in CH_3CN, T = 25 °C. □ = **2**, △ = **3**, ○ = **4**, ◆ = **5**, ▼ = **6**, ▲ = **7**. Solid lines are a best-fit to eq 3 to obtain K_{app}. Values for K_{app} are tabulated in Table 2.

Table 2. Equilibrium Data for Binding **2**−**8** with Mg(15-crown-5)$(Otf)_2$[a]

ligand	K_{app}	K_b (M^{-1})[c]
2	27(3)	1.7×10^3
3	22(7)	1.4×10^3
4	25(3)	1.6×10^3
5	5.0(3)	3.1×10^2
6	0.078(4)	4.9
7	0.38(4)	23.7
8	0[b]	0[b]

[a] In CH_3CN at 25 °C. [b] No binding observed. [c] $K_b = K_{app}/(K_{i(1)})$.

$$Q = \frac{K_{app}(1 + x) - [(K_{app}(1 + x))^2 - 4(K_{app} - 1)\,K_{app}x]^{1/2}}{2(K_{app} - 1)} \quad (3)$$

$$x = [Mg(15\text{-crown-5})]_{tot}/[L]_{tot}$$

The NMR, infrared, and conductivity data on solutions of **2**−**8** with Mg(15-crown-5)$(Otf)_2$ are consistent with the binding equilibria in Scheme 4. The binding constants K_{app} and K_b show a clear trend, with the strongest binding ligands being those having an unfunctionalized 2-imidazolidone ring, that is, **2**−**4**. N-methylation decreases K_{app} by a factor of 5, and N,N'-dimethylation decreases it by 350-fold. The decrease in binding free energy upon protection of the ureido nitrogens prompted us to speculate that the −NH group may substantially contribute to the binding enthalpy, ΔH_L, for L. Weak intramolecular hydrogen bonding would be consistent with the 0.6 ppm downfield shift in the −NH resonance upon binding to Mg(15-crown-5)$^{2+}$. The crystal structures of magnesium urea complexes[14] do reveal a general propensity for the ligated urea

Scheme 5

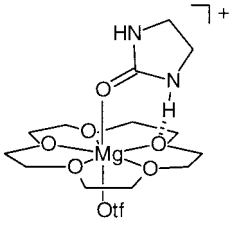

to interact with hydrogen bond acceptors coordinated -*cis* to it via interligand hydrogen bonds. A similar interaction is possible between the coordinated urea and an oxygen on the macrocyclic ring of Mg(15-crown-5)(Otf)$^{2+}$ as shown in Scheme 5, which would stabilize the adduct thermodynamically and kinetically.

This structural hypothesis prompted an analysis of the measured binding constants in the context of Scheme 5. Equation 4 relates the binding constant K_b for ligands **3** and **6**, $K_{b(3)}$ and $K_{b(6)}$, to the enthalpic and entropic components of the Gibbs free energies, ΔG_3 and ΔG_6. Beginning with the reasonable assumption that the entropic component is nearly the same for binding **3** or **6**, that is, $\Delta S_3 - \Delta S_6 \approx 0$, we obtain Eq 5 relating the binding constants for **3** and **6** to the difference in binding enthalpy, $\Delta H_3 - \Delta H_6$.

$$\Delta G_3 - \Delta G_6 = (\Delta H_3 - \Delta H_6) - T(\Delta S_3 - \Delta S_6) = -RT\ln(K_{b(3)}/K_{b(6)}) \quad (4)$$

$$-RT\ln(K_{b(3)}/K_{b(6)}) = \Delta H_3 - \Delta H_6 \quad (5)$$

Experimental values for $K_{b(3)}$ and $K_{b(6)}$, Table 2, give $\Delta H_3 - \Delta H_6 = 3.3(2)$ kcal/mol from Eq 5. This difference in binding enthalpy for **3** and **6** is within the range expected for a weak hydrogen bonding interaction and supports the theory that a primary factor affecting the binding equilibrium in **2**−**8** is their relative hydrogen bonding ability. This requires that the contribution of the carbonyl oxygen to binding enthalpy be comparable in **3** and **6**, an assumption strengthened by comparison of the metal binding constants for substituted ureas and thioureas. These data show that for binding to simple metal cations, the stability constants are essentially invariant with N-alkyl substitution.[21] Therefore, the primary difference in **3** and **6** is that both amido sites in **6** are blocked from hydrogen bonding, and the binding constants for **3** and its N,N'-dimethylated counterpart **6** should be related by the strength of the hydrogen bond with the former. This is consistent with the binding mode shown in Scheme 5, in which binding the carbonyl oxygen to the Mg^{2+} center in a bent fashion typical of urea complexes places the −NH group in position to hydrogen bond with one of the macrocycle oxygen atoms.

The complex with the unsymmetrical ligand **5** provides additional evidence for Scheme 5. Ligand **5** has two possible orientations when bound to Mg(15-crown-5)$^{2+}$, as shown in Figure 7 (inset). This is revealed in the NMR spectra of Mg(15-crown-5)(**5**)(Otf)$^+$ measured at −45 °C, Figure 7. A large −NH signal for Mg(15-crown-5)(**5**)(Otf)$^+$, **a**, is observed at 5.67 ppm, while the signal from free **5** appears at 5.11 ppm (not shown). The small signal at 5.58, which begins to appear only in spectra below 10 °C, is interpreted to arise from an alternate

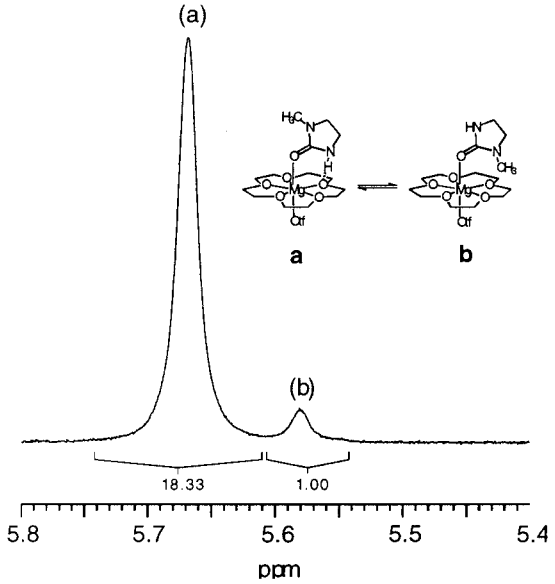

Figure 7. Low-temperature NMR spectra (400 MHz, CD_3CN, −45 °C) of Mg(15-crown-5)(Otf)(**5**)$^+$. Inset shows the structural isomerism proposed to give rise to signals (a) and (b). The spectra were measured in the presence of an excess of tetrabutylammonium trifluoromethansulfonate to ensure that a single Otf$^-$-ligated complex was formed.

coordination mode **b** in which ligand **5** has been rotated by 180° and the hydrogen bond with the macrocycle has been broken. We first define an equilibrium constant $K_{iso} = [\mathbf{a}]/[\mathbf{b}]$ for the isomerization equilibrium **a** ⇌ **b**. Then using the ratio of the intensities of signals (a) and (b), we calculate $K_{iso} = 0.051(4)$. By analogy with the previous argument, the position of the equilibrium established between **a** and **b** should be reflective of the strength of the hydrogen bond formed in **a**. Since $T\Delta S$ for the isomerization in CH_3CN is reasonably expected to be small, $\Delta H_a - \Delta H_b = RT\ln K_{iso} = 1.35(7)$ kcal/mol. This enthalpic difference is in the range for a weak hydrogen bond that is broken when **5** is rotated by 180°, which also supports the existence of a hydrogen bond between the −NH group and a macrocycle oxygen atom.

While the hydrogen bonding ability of the −NH functionality is a driving influence in the formation of the complexes, the Lewis basicity of the carbonyl oxygen cannot be entirely neglected in understanding the binding constants in Table 2. Ligands **6** and **8** have similar physical structures, and neither can form hydrogen bonds of the type illustrated in Scheme 4. They have very different binding affinities, however. Though binding of **6** is weak, binding to **8** is immeasureably small under our conditions. This is a result of the poor Lewis basicity of the ketonic oxygen when compared to amido and ureido oxygen donors and is consistent with comparative gas-phase binding energies for acetone and *N*-methylacetamide[22] with Mg^{2+}.

The data and analysis on binding of ureido and related ligands to the Mg(15-crown-5)$^{2+}$ unit present a strong case that Mg(15-crown-5)$(Otf)_2$ binds cyclic ureas, including biotin, by a ditopic interaction involving the carbonyl oxygen and ureido −NH functional groups. We believe that the hydrogen bonding interaction results from the structurally complementary length of the Mg−O_{crown} bond to the C═O···HN− distance in the ligands, Scheme 2. However, the highly ionic character of the

(21) Martell, A. E.; Smith, R. M. *Critical Stability Constants*; Plenum Press: New York, 1977; Vol. 3.

(22) Peschke, M.; Blades, A. T.; Kebarle, P. *J. Am. Chem. Soc.* **2000**, *122*, 10440−10449.

Mg−O bond also ensures that a lone pair from the macrocycle oxygen is available for hydrogen bonding. The Mg(15-crown-5)$^{2+}$ unit therefore provides two points of contact with the bound ligand by positioning a Lewis acidic Mg^{2+} to interact with the carbonyl group and a Lewis basic oxygen atom to interact with the −NH group. This dual interaction is consistent with the preferential binding of ureido ligands unfunctionalized at the nitrogen atom and with the slow ligand exchange kinetics. Interligand hydrogen bonding in Mg(15-crown-5)$^{2+}$ complexes has been previously invoked as a cause for the very slow exchange kinetics of axial ligands from Mg(15-crown-5)$^{2+}$ complexes.[19] However, this seems unlikely for the simple axial ligands such as methanol that were tested, and we feel that a much stronger case for interligand hydrogen bonding is made in the present system.

In this structural context, it is useful to compare the coordination of biotin to Mg(15-crown-5)$(Otf)_2$ with the binding site in the biotin-binding RNA aptamer.[7] The aptamer utilizes a planar $Mg(OH_2)_4^{2+}$ unit to bridge the biotin ureido carbonyl group to the phosphate backbone of the RNA. Therefore, the biotin and anionic phosphate moiety are ligated in *-trans* coordination sites on the Mg^{2+} ion. Recognition of the ureido headgroup by the aptamer is further enhanced by N^1H hydrogen bonding interactions to both Mg^{2+}-coordinated water molecules and an interstitial water molecule. These secondary interactions are similar to those observed in the biotin-Mg(15-crown-5)$^{2+}$ adducts, in which biotin is coordinated in an axial site and intramolecular hydrogen bonding contributes to the recognition of the biotin headgroup.

The structures of the Mg(15-crown-5)(**2**)$(Otf)^+$ adduct and the RNA-biotin complex suggest a hypothesis for activation of biotin for carboxylation in BDC enzymes. This would first involve coordination of biotin to the metal ion, which should have the effect of making the biotin headgroup more acidic by stabilizing its conjugate base anion. Carboxylation of biotin can be achieved through proton transfer to a suitably oriented basic residue followed by addition of CO_2 to the ureido anion. This is reminiscent of the function of the magnesium ion in RubisCO, where it stabilizes formation of an enediolate carbanion equivalent that is subsequently carboxylated by CO_2.[23] It is stressed here that the terminal enzymatic substrates in the biotin enzymes do not appear to bind to the metal ions during turnover,[24] but no spectroscopic or structural studies presently preclude the possibility that the biotin cofactor coordinates to a metal ion during enzyme turnover. To address the prospect that metal coordination may play a role in synthetic and perhaps biochemical biotin carboxylation processes, we are now characterizing proton-transfer reactions of cyclic ureas bound to Mg(15-crown-5)$^{2+}$ to determine whether it facilitates proton transfer and carboxylation of the ureido group.

Summary

We have presented data showing that the simple complex Mg(15-crown-5)$(Otf)_2$ binds to cyclic ureas through a bifunctional binding mode. Mg(15-crown-5)$(Otf)_2$ was shown to have a high affinity for biotin and to function as a receptor for the biotin headgroup. This results from chemical and structural complementarity between the $Mg-O_{crown}$ bonds and the ureido headgroup. Binding constants for a series of cyclic ureas were interpreted in terms of Scheme 5, in which hydrogen bonding with the macrocycle plays a critical role in stabilizing the Mg(15-crown-5)$(L)^{2+}$ adducts in solution. These data provide a chemical rationale for using the magnesium−oxygen bond as a general design component for the recognition of biotin. The interaction of the carbonyl oxygen of the ureido group with a Lewis acid may also provide a route to chemical activation of biotin. The solution structure was therefore analyzed as a model for noncovalent interactions with specific sites on biotin, which may be important to the carboxylation of biotin in BDC enzymes.

Acknowledgment. The National Science Foundation is acknowledged for a grant to M.T.C. (CHE-9985266), for an REU Fellowship to MCG (DBI 9988027), and for contribution toward the purchase of single crystal instrumentation used in this study (CHE 9808440). Dr. Mike Williams is acknowledged for assistance in collecting the low-temperature NMR data.

Supporting Information Available: Crystallographic data file for Mg(15-crown-5)$(Otf)_2$ (CIF), and derivations of eqs 1 and 3 (PDF). This material is available free of charge via the Internet at http://pubs.acs.org.

JA016641R

(23) Andrews, T. J. *Nat. Struct. Biol.* **1996**, *3*, 3−7. Cleland, W. W.; Andrews, T. J.; Gutteridge, S.; Hartman, F. C.; Lorimer, G. H. *Chem. Rev.* **1998**, *98*, 549−561.

(24) Mildvan, A. S.; Scrutton, M. C.; Utter, M. F. *J. Biol. Chem.* **1966**, *241*, 3488−3498. Fung, C. H.; Mildvan, A. S.; Allerhand, A.; Komoroski, R.; Scrutton, M. C. *Biochemistry* **1973**, *12*, 620−629. Fung, C.-H.; Mildvan, A. S.; Leigh, J. S., Jr. *Biochemistry* **1974**, *13*, 1160−1169.

(25) Bates, H. A.; Rosenblum, S. B. *Tetrahedron* **1984**, *41*, 2331−2336.